

Indicator Functions Detect Tangentially Transient Behaviour on Decaying Normally Hyperbolic Invariant Manifolds

Francisco Gonzalez Montoya ^{*1,2,3} and Christof Jung ²

¹Faculty of Physical Sciences and Engineering, University of Leeds, Leeds, LS2 9JT, United Kingdom

²Instituto de Ciencias Físicas, Universidad Nacional Autónoma de México, Av. Universidad s/n, Col. Chamilpa, Cuernavaca, Morelos, CP 62210, México

³Facultad de Ciencias, Universidad Nacional Autónoma de México, Av. Universidad 3000, Circuito Exterior s/n, Coyoacán, CP 04510, Ciudad Universitaria, Ciudad de México, México

January 7, 2025

Abstract

We study the decay scenario of a codimension-2 NHIM in a three degrees of freedom Hamiltonian system under increasing perturbation when the NHIM loses its normal hyperbolicity. On one hand, we follow this decay in the Poincaré map for the internal dynamics of the NHIM. On the other hand, we also follow the decay in a time delay function calculated on a 2-dimensional plane in the phase space of the system. In addition, we observe the role of tangential transient effects on the decaying NHIM and their manifestation in the delay time indicator function. Thereby we obtain ideas on how the decay of NHIMs and the tangential transient effects are encoded in indicator functions. As an example of demonstration, we use the motion of an electron in a perturbed magnetic dipole field.

1 Introduction

The global dynamics of a chaotic dynamical system is governed to a large extent by its unstable invariant subsets in the phase space, in particular by the ones of codimension 2. These subsets have stable and unstable manifolds of codimension 1 which can form walls and tubes in the phase space which direct the general dynamics. These considerations of codimensions hold equally well for the constant energy manifold of Hamiltonian flows as for the corresponding Poincaré maps. A remarkable kind of invariant sets in the phase space are normally unstable invariant surfaces known under the name “Normally Hyperbolic Invariant Manifolds”, standard abbreviation NHIMs. For general properties of these manifolds see [1].

For any important subsets in a phase space, the question of their stability always arises under general perturbations of the system. For NHIMs, the following persistence theorem holds: NHIMs survive perturbations and keep their global topology as long as their normal instability remains larger than their tangential instability. This property is called “normal hyperbolicity”. Several methods to prove the persistence theorem of NHIMs are developed in the references [1, 2, 3, 4]. Examples indicate that NHIMs start to decay locally as soon as in some point on the NHIM the tangential instability becomes larger than the normal instability. For three instructive examples see Figs. 4 and 5 and their explanation in [2], example 1.1 with Fig.1.3 in subsection 1.2.1 of [4], and Fig.9 and its explanation in section 6 of [5].

The persistence theorem does not imply the structural stability of the internal dynamics of the NHIMs. Under general perturbations, we find qualitative changes of the internal dynamics and in particular bifurcations of the important internal periodic orbits within the NHIMs. These changes also include the creation of chaos in the internal dynamics. However, according to the persistence theorem the NHIM survives and keeps its topology as long as the normal hyperbolicity property is conserved. The development scenario of the internal dynamics of a NHIM under any perturbation can be investigated and presented graphically best by the restriction of the Poincaré map to the NHIM.

In the following, we are interested in Hamiltonian systems with 3 degrees of freedom (3-dof). They have a complete phase space of dimension 6, a constant energy manifold of dimension 5, and Poincaré maps acting on domains of dimension 4. Therefore, the most interesting invariant subsets in the constant energy manifold are the ones of dimension 3, and they correspond to invariant surfaces of dimension 2 in the domain of the Poincaré map. In most cases, it is simpler to argue for maps than for flows. Therefore in this article, we will present our ideas mainly for maps. For 3-dof systems the codimension-2 NHIMs in the map are 2-dimensional and then the map of their internal dynamics can be displayed by 2-dimensional graphics. We use this graphical representation extensively in the present article.

*f.gonzalezmontoya@leeds.ac.uk,
f.gonzalez.montoya@ciencias.unam.mx

Some investigations of the loss of normal hyperbolicity of NHIMs have been reported in [6, 7, 8, 9]. These examples either use 2-dof systems or use simplifications which are equivalent to a reduction of the problem to 2 degrees of freedom. They are mainly concerned with the implications of the loss of normal hyperbolicity to transition state theory and transport problems. They are less concerned with the remnants of the NHIMs during their decay to fragments which are partially of lower dimensions, a problem with which we are concerned in the present article. For further interesting publications on changes of NHIMs and their invariant manifolds under parameter changes see also [10, 11, 12, 13, 14, 15, 16].

In the present article, we deal with the problem of the disintegration of NHIMs when they lose their normal hyperbolicity and with the problem of how we observe this decay. We investigate the remaining fragments numerically with the help of phase space structure indicator functions. Therefore let us give here some basic introductory remarks on indicator functions.

When a 0-dimensional unstable invariant set, i.e. a hyperbolic fixed point of a map, collides with a stable fixed point and runs through a saddle-center bifurcation then it disappears completely from the domain of the map. Using the normal form approximation of the map around the hyperbolic equilibrium point, we can observe how these fixed points disappear into the complex generalization of the domain of the map.

First, we consider a set of parameter values where the unstable fixed point still exists and let us discuss what we observe in indicator functions. The most appropriate indicator function for this purpose is the time delay function which indicates the time during which a general trajectory stays in some neighbourhood of the unstable fixed point. If the trajectory starts exactly on the stable manifold of the fixed point, then this trajectory converges to the fixed point, it stays in the neighbourhood of the fixed point for an infinite future and accordingly, the time delay diverges. When it starts not exactly on the stable manifold but close to it, then this trajectory comes close to the fixed point, stays in its neighbourhood for some time but leaves this neighbourhood again after a finite time and accordingly, the time delay is large but finite.

If we plot this time delay over some surface of initial conditions in the phase space then we detect the intersections between the stable manifold of the fixed point and this surface. This basic idea also works for the detection of stable manifolds of higher dimensional unstable invariant subsets and it is the basic idea of how we search for NHIMs numerically, for all the details see [17].

For a 0-dimensional unstable fixed point, the invariant set disappears at once completely in a single bifurcation at one specific value of the perturbation parameter. For higher dimensional invariant subsets the decay of the invariant set is a process which starts at a particular value of the perturbation parameter. Then the decay continues over some possibly large interval of the perturbation parameter. Parts of the original 2-dimensional NHIM surface remain while other parts decay and leave behind only a (in general fractal) collection of fragments which partially have lower dimensions than the original NHIM. In the most extreme case, the NHIM in the map turns into a fractal powder only, for an example of such a scenario see [5].

In the time delay function, we recognise these events as follows, when we construct the indicator function on a 2-dimensional domain, i.e. on a surface of codimension 2 in the domain of the map. The stable manifold of the NHIM in the map is a fractally folded submanifold of dimension 3 before the beginning of the decay. So its transverse intersection with a codimension 2 surface is a fractal collection of 1-dimensional curves. Surviving parts of the NHIM also give these results after the start of the decay.

In contrast look at decaying parts. Here the NHIM surface decays into lower than 2-dimensional parts, let us look at a particular part with a (maybe fractal) dimension k . Their stable manifolds have dimension $k + 1$. The transverse intersection of these stable manifolds with the 2-dimensional intersection surface over which we plot the indicator function has dimension $k - 1$. In particular, if $k < 1$ then this intersection is empty in general. That is, we do not see any corresponding singularities in the plot.

However, when we start in regions close to some remnants of the stable manifolds of the NHIM then there is some large but finite time delay compared with other regions nearby. The effect looks as if the infinite singularities of the indicator function are removed and only a high background is left. If there is a fractal collection of remnants, then the time delay function has a lot of finite maxima which gives this function a complicated appearance. For a previous observation of this type of complicated behaviour in a time delay function along a 1-dimensional line of initial conditions see [18].

These results form a new type of transient behaviour which shows an interesting contrast to the usual transient behaviour near unstable invariant subsets. For a NHIM before the beginning of any decay, we are used to the following behaviour. A general trajectory comes close to the invariant subset moving near the stable manifold of this subset. Then it stays near the invariant subset for some finite time and leaves the neighbourhood of this subset again moving close to the unstable manifold of this unstable invariant subset. While close to the invariant subset the general trajectory performs a type of motion very similar to the motion of trajectories within the invariant set. This is the usual type of transient behaviour, see [19]. So we have transient dynamics in the normal direction of the NHIM and this usual transient motion continues also during the decay of the NHIM.

However, when the NHIM starts to decay, we find in addition also some kind of transient behaviour in the tangential direction of the NHIM. This can be understood along the following considerations. Usually, a NHIM which did not yet start its decay is compact, and then a trajectory belonging to the NHIM can not leave the NHIM. In addition, a trajectory very close to the NHIM can not leave the neighbourhood of the NHIM in the tangential direction. It will do so only in the normal direction.

This situation changes fundamentally as soon as the NHIM starts its decay. Then a general trajectory belonging to the NHIM and not moving on a regular substructure can approach the boundary of decay by tangential motion on the NHIM. It can finally cross this boundary also by tangential motion along the surface which has belonged to the NHIM before the beginning of the decay. After the beginning of the decay, such regions are the logical continuation of the surviving parts of the NHIM in the tangential direction. Thereby this general trajectory is lost from the neighbourhood of the remaining pieces of the NHIM.

Finally, we consider a general trajectory which approaches the neighbourhood of the NHIM by motion close to its surviving parts of the stable manifold. Then this trajectory in the neighbourhood of the decaying NHIM has two competing possibilities to leave the neighbourhood of the surviving parts of the NHIM again. First, it can leave along the unstable manifolds of the surviving parts of the NHIM. Second, it can move mainly tangentially to the NHIM over the boundary of decay and leave the surviving parts of the NHIM along this direction. Or more generally it can leave by a combination of these two routes.

In this article, we treat the case of 3-dof systems and NHIMs of dimension 2 in the map. When such a NHIM starts to decay then we find surviving parts of 2-dimensional surfaces. In the general case, the internal dynamics of such parts contain KAM curves and chaos layers. Then the interior of KAM curves (and this includes chaos layers inside) are trapped on these surviving parts of the NHIM forever.

As a short side remark let us mention briefly the essential differences which we find for systems with even more degrees of freedom, let us say $k > 3$ in number. Then the dimension of the domain of the map is $2k - 2$. Now assume that we have a codimension 2 NHIM, i.e. it has dimension $2k - 4 > 2$ in the map. There are still KAM curves of the internal dynamics of the NHIM. And we have chaos layers. However, for $k > 2$, we have Arnold diffusion in the internal dynamics of the NHIM, all the chaos layers are interconnected and a general trajectory starting in some fine chaos layer in the long run can diffuse over the whole chaotic part of the internal dynamics.

Now assume that the decay of the NHIM has started in some part. The boundary of the decay has contact with this global chaotic part. And accordingly, all the trajectories starting in the chaotic part will cross the boundary of the decay in the long run. In this sense, there are no surviving parts of the NHIM of the full dimension $2k - 4$ as soon as the decay has started in some part of the NHIM. All the remnants of the NHIM are a collection of lower dimensional subsets only. This is qualitatively different from the case of NHIMs of dimension 2, where we find surviving parts of the full original dimension.

In this work, we take the motion of a charged particle in a perturbed magnetic dipole field as an example of demonstration. The perturbation is the addition of a quadrupole contribution to the magnetic field. This example has one unusual property. Namely, the decay of the NHIM starts as soon as the perturbation parameter, and the magnitude of the quadrupole contribution becomes different from 0. So we do not have some interval of the perturbation parameter, where the NHIM persists in the topology which it had for perturbation 0. However, this is no problem for the topic of the present article, since we are interested in the decay of NHIMs anyway. Otherwise, this magnetic dipole example is an excellent and typical example to study the decay scenario of a NHIM. Details of our previous studies of this magnetic dipole example and many further references for this system can be found in [20].

The present article is organised as follows: In section 2, we present the basic dynamics of our example of demonstration, in particular, the construction of the main NHIM and its stable and unstable manifolds. In section 3, we show the plots of the indicator function, i.e. the time delay function, and for comparison also the corresponding plots of the Poincaré map restricted to the NHIM. Section 4 contains our conclusions and some final remarks.

2 Example: The motion of an electrically charged particle around a perturbed magnetic dipole

As an example of demonstration for the disintegration of a NHIM and for the creation of corresponding tangential transient effects, we treat the motion of an electrically charged particle in the field of a magnetic dipole perturbed by a magnetic quadrupole. The Hamiltonian function of the system in cylindrical coordinates (r, ϕ, z) is given by

$$H = \frac{1}{2m} \left(\vec{p} - \frac{q}{c} \vec{A} \right)^2 = \frac{1}{2m} \left(p_r^2 + \left(\frac{p_\phi}{r} - A_0 \frac{r}{(r^2 + z^2)^{3/2}} \right)^2 + \left(p_z - \epsilon \frac{r^2 \sin 2\phi}{(r^2 + z^2)^{5/2}} \right)^2 \right). \quad (1)$$

Here A_0 is the magnitude of the magnetic dipole moment which is aligned in the z direction. The term in Eq.1 containing A_0 is the magnetic dipole potential. And ϵ is the magnitude of the quadrupole perturbation of the field, which serves as a perturbation parameter in the investigation of the development scenario of the NHIM M of this particular system. The term in Eq.1 containing ϵ is the magnetic potential of one particular quadrupole component. The phase space of the full system is 6-dimensional and has the coordinates $(r, p_r, \phi, p_\phi, z, p_z)$.

The dipole potential has a rotational symmetry around the z -axis and correspondingly under the influence of the dipole field only, i.e. in the unperturbed case $\epsilon = 0$ the z -component of the angular momentum of the particle, i.e. $L_z = p_\phi$, is conserved and it acts as if it would be a parameter of the system. In this case, the system reduces to a 2-dof system. For the quadrupole field, we have chosen a component which is not symmetric around the z -axis such that for $\epsilon \neq 0$ the angular momentum L_z is no longer conserved. In this case, the system can no longer be reduced to a 2-dof system.

In the next section, we show numerical results for the perturbation of the system where we start with the unperturbed case of $\epsilon = 0$ and then increase ϵ slowly to observe the effects of the perturbation away from the partially integrable case. Let us denote as M_0 the NHIM of the system for the unperturbed case and M_ϵ the NHIM for the perturbed case. In particular, we will study the change of the NHIM M_ϵ of the system under this perturbation. Therefore, it is important to understand the structure of the NHIM M_0 well in the unperturbed case. For $\epsilon = 0$, the 6-dimensional phase space of the complete 3-dof system foliates into a continuum of 2-dof systems, one for each possible value of the conserved quantity L_z . The phase space of each one of these reduced 2-dof systems is a copy of the 4-dimensional space of the variables (r, p_r, z, p_z) .

Accordingly, the full 6-dimensional phase space is a Cartesian product of a circle representing the cyclic angle ϕ with the pile of the 4-dimensional phase spaces of the reduced 2-dof systems. During this pile construction the pile parameter L_z takes over its role as a phase space coordinate of the full 3-dof system.

Having this pile construction in mind it is easy to imagine the structure of the NHIM M_0 of the unperturbed full 3-dof system. First, let us consider one particular value of the total energy E . This cuts out a 5-dimensional surface of the full phase space and a corresponding pile of 3-dimensional energy surfaces of the reduced 2-dof systems.

This pile construction also induces a pile construction of the Poincaré map and a foliation of its 4-dimensional domain into 2-dimensional leaves belonging to the various values of L_z . Now imagine that the reduced Poincaré map has a hyperbolic fixed point which exists for some interval of L_z values. In the pile construction this continuum of fixed points forms a continuous line of points and by the formation of the Cartesian product with the circle representing the cyclic angle ϕ it forms a 2-dimensional surface with the topology of a cylinder segment. This surface is invariant by construction and it inherits normal hyperbolicity from the hyperbolicity of the fixed point in the reduced system. Thereby this surface is the NHIM M_0^P of the unperturbed partially integrable system in the 4-dimensional domain of its Poincaré map.

In the particular example of the system defined by Eq.1 the normal hyperbolicity of the unperturbed NHIM M_0^P vanishes at one boundary of the cylinder segment and thereby it is clear that any perturbation of the partial integrability of the system triggers the decay of this NHIM M_0^P surface beginning from this boundary with vanishing normal hyperbolicity. Therefore this dipole example is an ideal system for studying the events occurring during the decay of a NHIM M_0 under well-controlled conditions. For more details on all these considerations including detailed numerical illustrations see [17, 20] and references therein.

3 Decay of the NHIM: Numerical Results for the Delay Time and for the Poincaré Map

The delay time is a natural tool to study the phase space of open Hamiltonian systems. In general, the phase space structure indicators are useful to visualize invariant manifolds in the phase space. In particular, they are useful to find KAM islands, unstable and stable manifolds of NHIMs and to obtain information on their bifurcations when we change the parameters in the system. The details of the ideas of phase space structure indicators like the fast Lyapunov indicator, Lagrangian descriptors, Birkoff averages, the classical action, and delay time can be found in the references [21, 22, 23, 24, 25, 26, 20]. For more information on the recent developments in this topic see the references contained in [27, 28].

The delay time t_d as a phase space structure indicator is defined as the sum of two parts, the time delay t_d^+ calculated forwards and the time delay backwards t_d^- .

$$t_d = t_d^+ + t_d^- = \tau - \frac{r^+ - r_0}{v^+} + \tau - \frac{r^- - r_0}{v^-}. \quad (2)$$

Where r_0 is the distance of the initial point to the origin at the initial time, r^+ the distance at the time τ of the forward integration, r^- the distance at time τ of the backward integration, and v^+ and v^- are the asymptotic velocities of the particle. For this Hamiltonian system, both velocities coincide $v^+ = v^-$. More details about the delay time as a phase space structure indicator are contained in the reference [20].

To visualize the decay of the NHIM M_0 and the transient behaviour of the trajectories, we break the rotational symmetry and calculate the time delay indicator on a surface of initial conditions that intersects the perturbed NHIM M_ϵ and its stable manifold. This phase space structure indicator is a natural choice for open systems. It gives us direct information on the trajectory's behaviour. If the trajectories are close to the bounded invariant chaotic set, then their time delay is larger compared to the other trajectories not approaching the invariant set. Only the trajectories on the fractal chaotic set generated by the stable and unstable manifolds of the NHIM M_ϵ and the ones in the stable KAM tori stay trapped in the interaction region forever.

First, we consider the unperturbed system as a reference for studying the perturbed case. We take initial conditions on the $r-L_z$ plane at $z = 0$, $p_r = 0$, and $\phi = 0$ for the fixed value of the energy $E = 0.05$, and calculate the time delay. The results are shown in the Fig.1 on the colour scale. The blue regions correspond to low escape time, the trajectories with those initial conditions escape to the asymptotic region faster than the other regions. The yellow-green fractal corresponds to the intersection of the homoclinic tangle of the NHIM M_0 and its stable manifolds with the set of initial conditions. The yellow region with low values of L_z are the intersections with the stable manifolds of the KAM islands, those trajectories on the invariant sets are trapped forever. The right border of this fractal corresponds to

the NHIM M_0 . For more information on the bifurcation diagram of the unstable periodic orbits and stable periodic orbits of the system see Fig.1 (b) in reference [20].

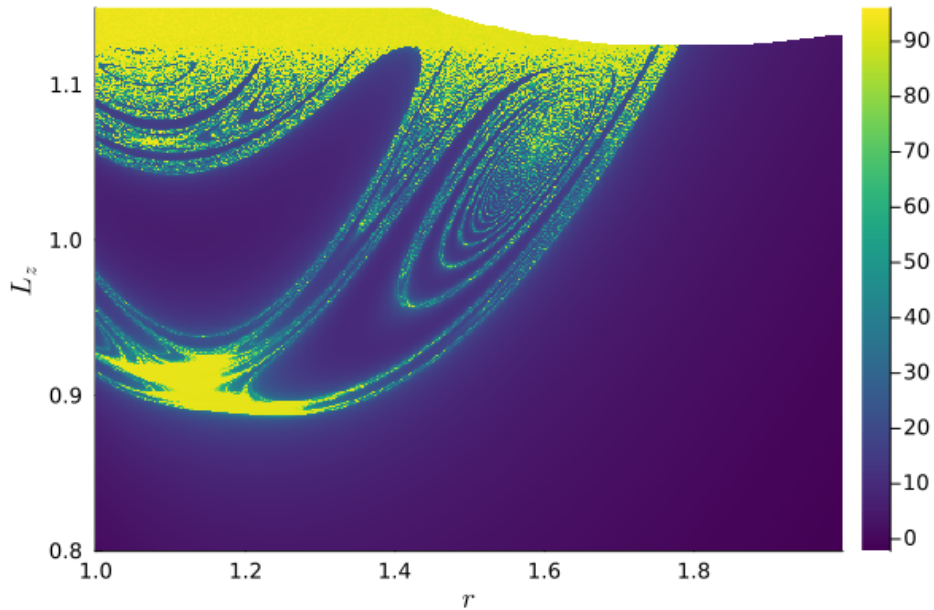


Figure 1: Time delay indicator on colour scale for the unperturbed case, $\epsilon = 0$ (see the homoclinic tangle formed by the stable and unstable manifolds of the NHIM M_0 in Fig.1 in [29] and Fig.2 in [17] for different values of L_z). The integration time $\tau = 500$.

To give an interpretation of the figures of the indicator function it is instructive to compare them with the corresponding plots of the inner NHIM M_0 structure. These plots are constructed by the following method: First, we construct the Poincaré map in the intersection surface $z = 0$ where the intersection orientation is irrelevant because of the reflection symmetry of the system in this intersection plane. Second, we restrict this map to the 2-dimensional NHIM M_0^P surface. Thereby we obtain the Poincaré map for the internal dynamics of the NHIM M_0 , which is a 2-dof dynamics corresponding to a Poincaré map having a 2-dimensional domain. In the following, we call this map of the internal dynamics of the NHIM “the restricted map”.

The Poincaré map of the NHIM M_0 has a 1:1 projection on the ϕ - L_z plane and therefore we show plots of the restricted map by this projection on the ϕ - L_z plane. As usual, we present the map graphically by showing many iterates of a moderate number of initial points, for more details see [20]. In Fig.2, we show this Poincaré map for the unperturbed case $\epsilon = 0$ and in the various parts of Fig.3 we show the perturbed Poincaré map for the same 4 values of ϵ which we will use in the various parts of Fig.4.

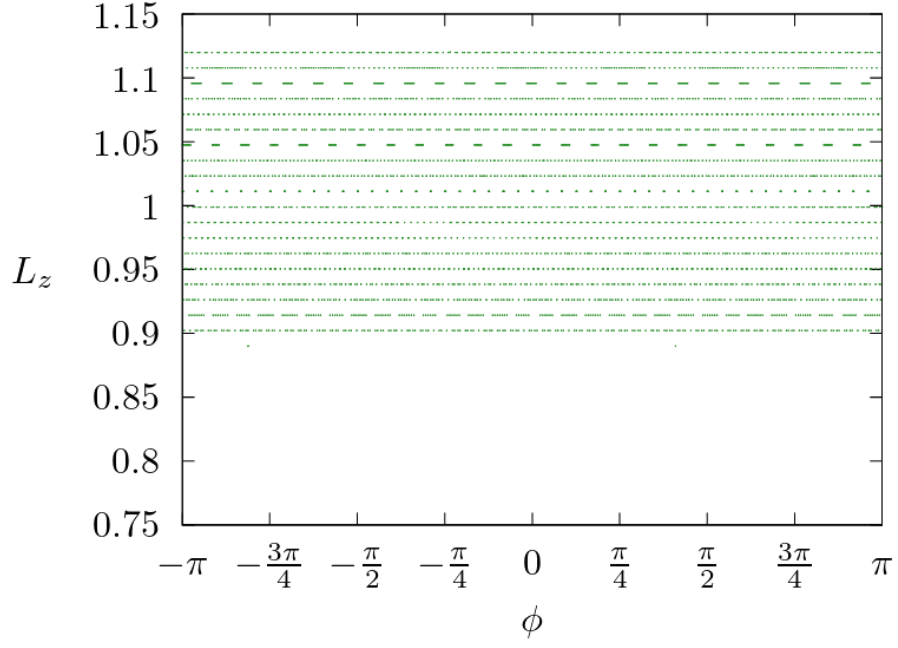


Figure 2: Poincaré map of the NHIM M_0 for the unperturbed case $\epsilon = 0$.

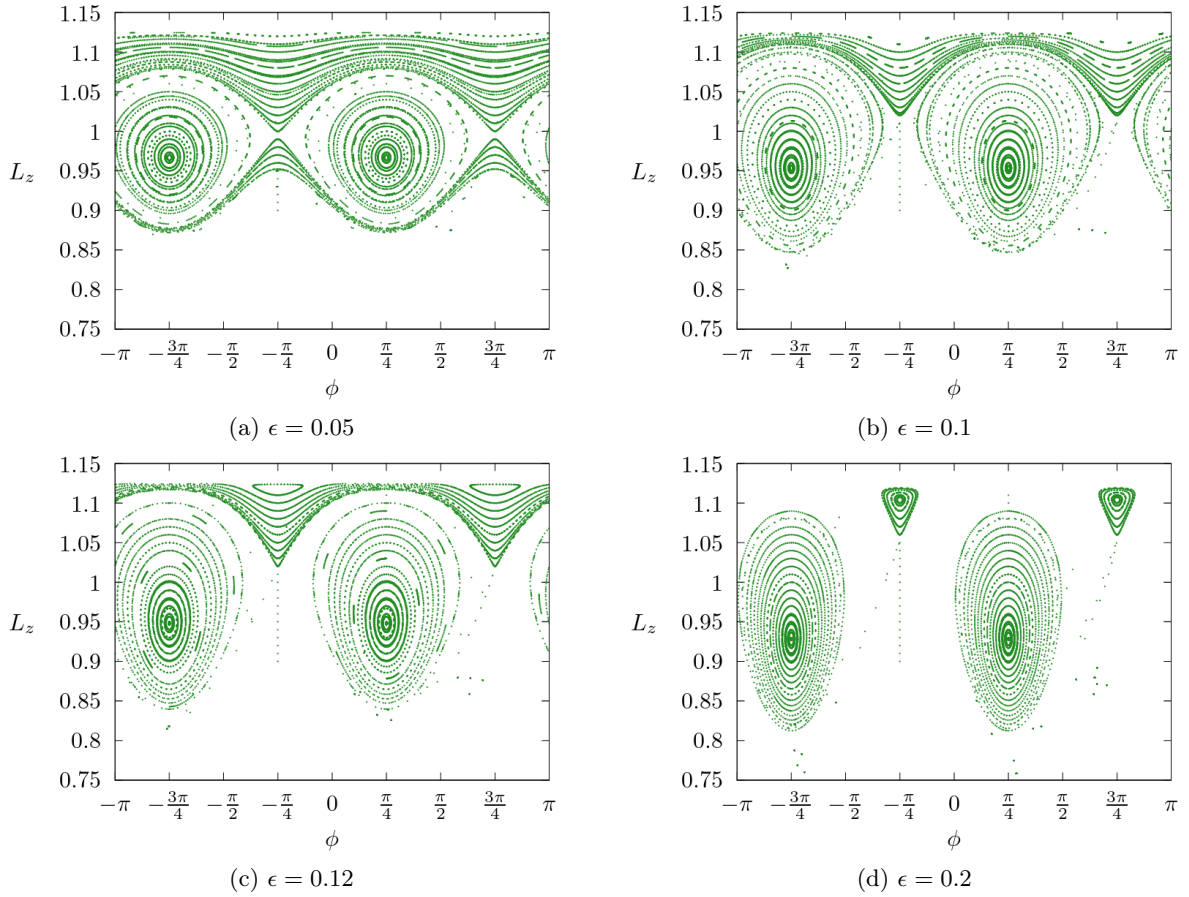


Figure 3: Poincaré maps of the NHIM M_ϵ for the perturbation parameter values $\epsilon = 0.05, 0.1, 0.12, 0.2$

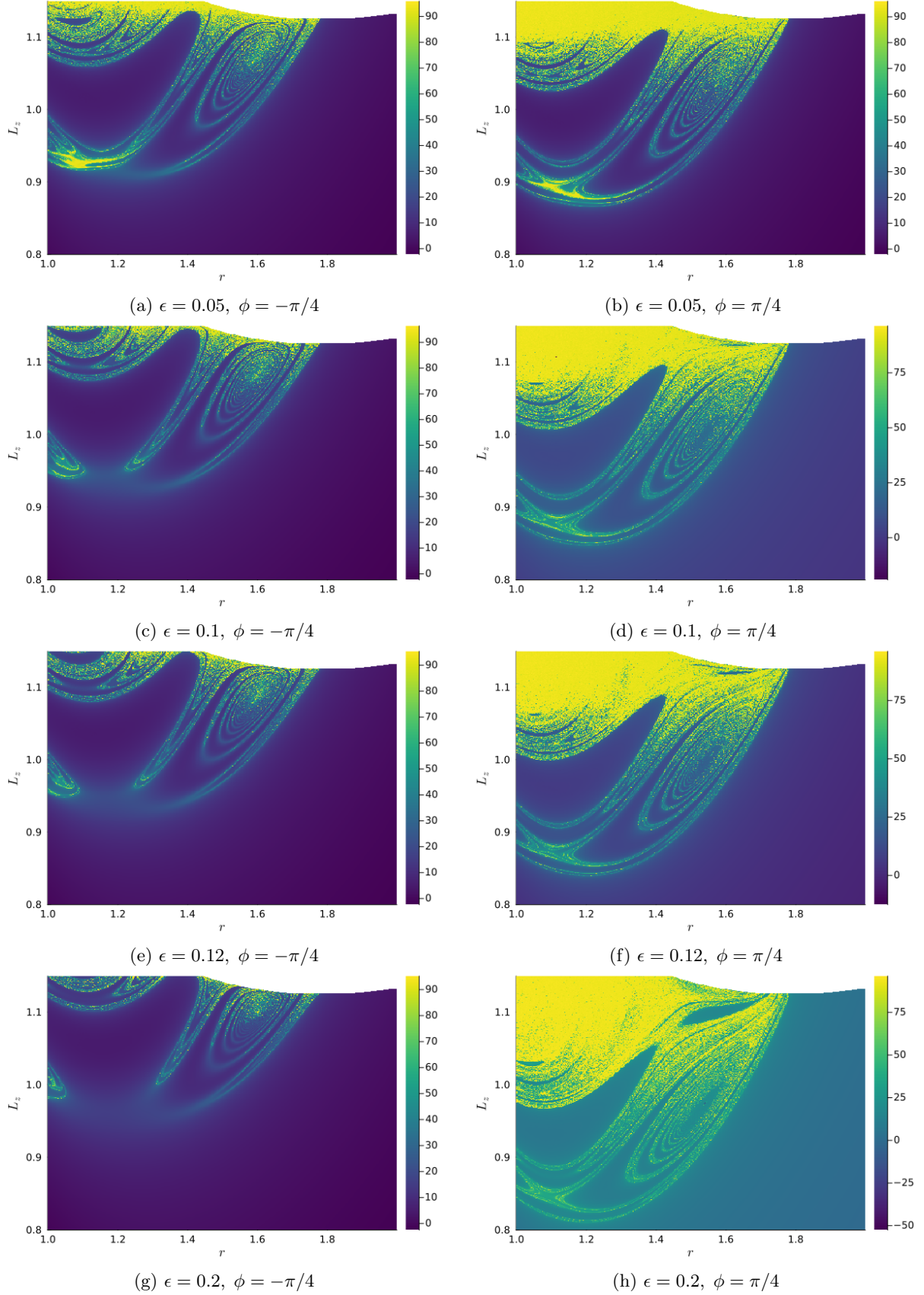


Figure 4: The time delay function plotted on the $r - L_z$ plane for the 4 values $\epsilon = 0.05, 0.1, 0.12$, and 0.2 of the perturbation parameter and for the 2 values $\phi = -\pi/4$ and $\phi = \pi/4$ of the azimuth angle. The integration time is $\tau = 500$. The value of the time delay is colour coded according to the right hand colour bar.

In Fig.2 for the unperturbed case $\epsilon = 0$ we see a foliation of the domain of the map into invariant horizontal lines of constant L_z . This is caused by the conservation of L_z for the rotationally invariant case of $\epsilon = 0$. As usual, under perturbations, the invariant lines with a rational winding number are broken and replaced by secondary island chains and chaos stripes whose width grows with increasing perturbation. The most prominent secondary structure is one of the islands centred at $L_z \approx 0.95$ and $\phi = \pi/4$ or $\phi = -3\pi/4$. To this secondary structure also belongs a separatrix

region with tangentially hyperbolic points near $L_z \approx 1$ and $\phi = -\pi/4$ or $\phi = 3\pi/4$. At the perturbation $\epsilon = 0.05$ this separatrix structure is still close to a separatrix line, see Fig.3 (a).

In Fig.3 (a) we also observe how the decay starts from small values of L_z . However, the decaying region is still separated from the separatrix structure mentioned above by primary KAM curves in between. For the internal dynamics restricted to the NHIM M_0 and therefore also for the restricted Poincaré map the KAM curves are impenetrable. Accordingly, the separatrix structure still is a truly invariant remaining part of the NHIM M_ϵ for such small perturbations.

The situation changes drastically for larger values of the perturbation. In Fig.3 (b) the KAM lines below the large secondary structure have already been broken and thereby the former separatrix structure has established contact with the decay front of the NHIM M_ϵ . Then strictly speaking the complete separatrix structure is no longer a remaining invariant part of the NHIM M_ϵ . Iterates of initial points from this separatrix region at first move chaotically inside of the separatrix structure. However after a sufficient number of iterations, they come close to the decay front, possibly cross it and leave the surviving NHIM M_ϵ surface tangentially.

To illustrate this effect pictorially several initial points on the line $\phi = -\pi/4$ have been chosen and their iterates are also included in the figure as long as these iterated points could be stabilized on the former NHIM M_ϵ^P surface by our method to construct the restricted map. See the irregularly scattered points in the former separatrix region and below the remaining large KAM islands. These trajectories have a transient existence on the remaining parts of the NHIM M_ϵ^P surface only.

For further perturbation increases, all primary KAM curves are destroyed and the only remaining and truly invariant parts of the NHIM M_ϵ^P are the surviving stable islands. This includes very tiny ones located inside of the region of the transient chaos. And now we have to see how this whole scenario is transferred to the indicator functions and observed in the corresponding plots.

First, we have to decide, on which 2-dimensional planes S we want to construct the indicator function to detect well the development scenario of the NHIM M_ϵ by the observation of time delays. According to the properties of the delay function already mentioned above in the introduction it must be assured that S intersects the stable manifold $W^s(M_\epsilon)$ of the NHIM M_ϵ . $W^s(M_\epsilon)$ is a surface of codimension 1, therefore a 2-dimensional plane in general position should intersect it transversally, as long as the plane lies close to the NHIM. Remember that the phase space coordinates z and p_z do not appear in the map.

This property can be assured along the following considerations. We have already mentioned that the NHIM surface projects 1:1 into the $\phi - L_z$ plane. And on the NHIM M_ϵ the coordinates r and p_r are always close to the values $r = 1$ and $p_r = 0$. Therefore the $r - L_z$ plane at $p_r = 0$ and at any value of ϕ should work well. With the Fig.3 in mind, we have chosen the two values $\phi = \pm\pi/4$ with the intention that the plot at one value should be heavily influenced by the big secondary islands and the other plot should emphasise the separatrix structure.

Keeping in mind that $W^s(M_\epsilon^P)$ has codimension 1 in the domain of the map and S has codimension 2, we expect that we obtain 1-dimensional intersections with $W^s(M_\epsilon)$ on the plane S . Accordingly, we expect singularities of the time delay function along these 1-dimensional lines of intersection. In addition, we can expect that S also has intersections with the 2-dimensional NHIM surface M_ϵ^P itself at least in isolated 0-dimensional points.

Globally $W^s(M_\epsilon)$ and $W^u(M_\epsilon)$ form homoclinic intersections and build up a chaotic tangle. Therefore the stable and unstable manifold form a fractal of tendrils. In the end, we have in S a fractal collection of 1-dimensional intersection lines with $W^s(M_\epsilon)$ leading to a fractal collection of lines of singularities of the time delay function. This is exactly what we see in Fig.1. Between the curves of singularities, the time delay drops to finite values. However in regions of a high density of lines of singularities with only very small gaps in between them also inside of the gaps we have rather high finite values of the time delay. In the plots, the whole region has obtained yellow colour. However, in a comparison between Figs.1 and 5, we see that under magnification we can resolve more gaps in the fractal intersection structure.

Next, we consider nonzero perturbations. We know already from the plots of the restricted map in Fig.3 that along $\phi = -\pi/4$ there is a lot of decay on the NHIM M_ϵ^P whereas along $\phi = \pi/4$ the NHIM M_ϵ^P forms a large island and thereby the NHIM M_ϵ^P surface survives. Accordingly on the indicator function in the plane along $\phi = \pi/4$ sharp fractal structures remain, even though they change in some details, whereas in the plane along $\phi = -\pi/4$ a considerable part of the former fractal structures is converted into a very diffuse region of still large but not infinite values of the time delay.

In the magnification in Fig.6 we observe that under a magnification no finer structure is resolved in the diffuse region. The delay function remains a very smooth distribution of high values only. There are no intersections with the stable manifold of an invariant surface leading to true singularities of the time delay. There is only a large region of initial conditions where trajectories run into the direction of the former NHIM M_ϵ surface and stay close to this region of already destroyed parts of the NHIM M_ϵ for a large but always finite time.

In the final part of this section, we point out some details of the delay plots which demonstrate how closely the indicator function follows the changes in the NHIM M_ϵ structure. In Fig.4 we also observe surviving clearly fractal structures for high values of L_z corresponding to the surviving parts of the NHIM M_ϵ^P at high values of L_z also for ϕ around $-\pi/4$. This parallelism explains in which way indicator functions can illustrate the decay scenario of NHIMs.

In Fig.1 we observe very high values of the time delay around $\phi = 1.2$, $L_z = 0.9$ representing a fractal of singularities which is not well resolved. Fig.5 shows that under higher resolution and a related rescaling of the colour bar, the plot still represents a fractal of singularities. The Figs. 4(a) and 4(b) show that these very high values of the time delay

survive the small perturbation of $\epsilon = 0.05$. The structures are only deformed and shifted a little. These structures in the delay functions are caused by initial conditions converging towards the separatrix structure along the part of $W^s(M_\epsilon)$ lying over the separatrix structure. Remember that according to the foliation theorem (chapter 5 of [?]) $W^s(M_\epsilon)$ transports the inner structure of the NHIM M_ϵ along it.

Next we increase the perturbation to the value $\epsilon = 0.1$ in Figs.4(c) and 4(d). Here the very high value of the time delay for $\phi \approx 1.2$ and $L_z \approx 0.9$ is no longer present. The better resolution under the magnification in Fig.6 shows that for this higher perturbation, the true singularities pointed out above are gone. We also observe that for $\phi = -\pi/4$ in Fig.4(c) the background value has dropped considerably whereas for $\phi = \pi/4$ in Fig.4(d) at least some higher background can be recognised. In this form, we get a clue that for smaller perturbations there has been some important structure present which becomes destroyed for increasing perturbation.

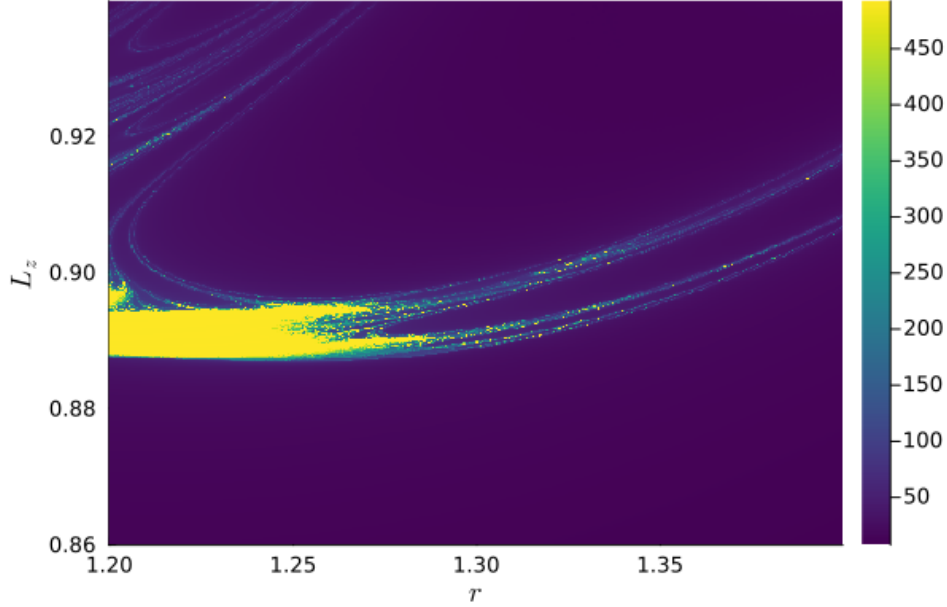


Figure 5: Magnification of the time delay indicator from Fig.1 on colour scale for the unperturbed case, $\epsilon = 0$. The integration time $\tau = 500$.

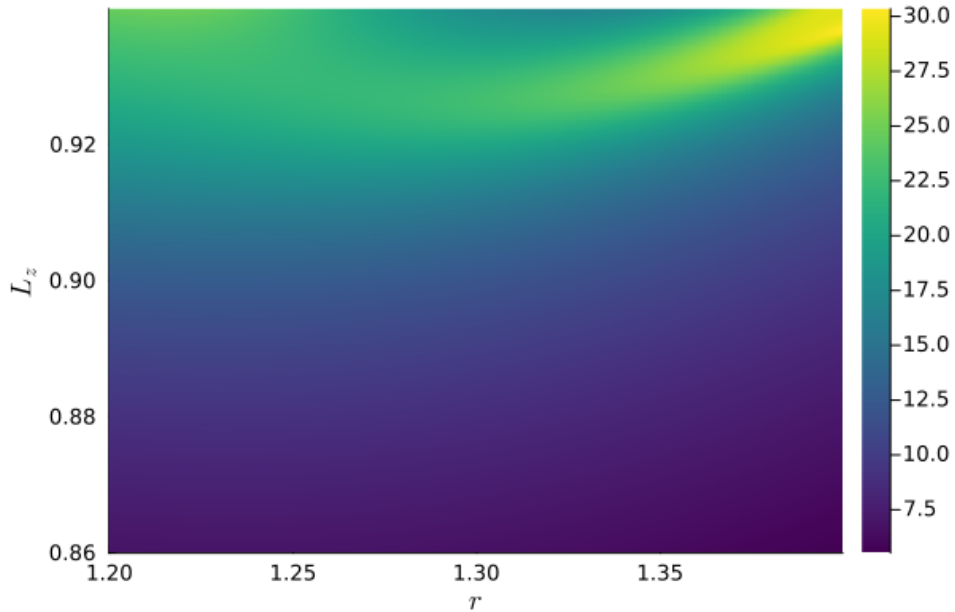


Figure 6: Magnification of time delay indicator from Fig.4 (c) at $\epsilon = 0.1$, $\phi = -\pi/4$. The integration time $\tau = 500$.

Finally, we point out some analogies between the indicator function and the Poincaré map in more detail. In Fig.2(a) we see that for $\epsilon = 0.05$ the large separatrix structure is still confined on both sides by primary KAM curves. It has not yet established any contact with the decay front. Therefore trajectories in this separatrix structure can not escape by tangential motion on the surviving parts of the NHIM M_ϵ . This statement is valid for all values of ϕ .

The situation is drastically different for $\epsilon = 0.1$. Here the separatrix structure has contact with the decay front. As we have already mentioned above, initial conditions in the separatrix region leave by tangential motion towards the decay front. Accordingly, the separatrix structure is no longer an invariant part of the NHIM M_ϵ and also the part of $W^s(M_\epsilon)$ over the separatrix structure no longer exists as a true stable manifold of an invariant subset.

By looking at Fig.3(b) it becomes understandable that initial conditions in the former separatrix region around $\phi = \pi/4$ and above the large secondary island needs a longer time to diffuse tangentially to the decaying front than the ones starting around $\phi = -\pi/4$. Accordingly, there still exist transient remnants of the stable manifold of the former separatrix structure near $\phi = \pi/4$ which also have influence on the indicator function when they intersect its domain in contrast to the behaviour around $\phi = -\pi/4$.

This explains why in Fig.4(d) we still observe long transients near $r = 1.1, L_z = 0.9$ in contrast to Fig.4(c) where we observe rather short transients only. A comparison between the whole scenarios of Fig.4 and Fig.3 makes it easy to understand why in total the transient effects fade out with increasing perturbation.

4 Conclusions and Remarks

The decay of the NHIM and the related tangential transient effects can be seen in the restricted Poincaré map and also in the time delay function used as phase space structure indicator function. Now the reader may ask what are the advantages and disadvantages of these two possibilities to display the scenario as a function of the perturbation strength.

The time delay function is easy and rapid to calculate and as any indicator function, it can be calculated and presented on any 2-dimensional surface in the constant energy manifold of the phase space. Moreover, it is not necessary to have detailed previous information on the location of the NHIM. The initial conditions leading to a high value of the time delay lie close to the stable manifold of localized subsets and guide us automatically towards the unstable invariant set.

In contrast, the construction of the restricted Poincaré map needs the approximate knowledge of the position of the NHIM to start the calculations. As explained in detail in [17] so far we use a numerical method which constructs the restricted map and searches for the position of the NHIM in a combined form. As long as we have small perturbations and complete NHIMs without decay this method works quite well and is reliable. This method can display the finest details of the internal NHIM dynamics in graphical form including tangentially chaotic parts. However, for large perturbations and NHIMs in the process of decay, the method becomes more difficult. In some examples (not yet published so far) it has become extremely difficult to find transient parts of the NHIM in the process of decay by this method. It needed a lot of numerical effort and needed the special adaption of the method for each individual transient substructure of the NHIM.

In this sense, the indicator function is the easier and more versatile method in general and it is also able to indicate the effects coming from the decaying parts of the NHIM. By relying on time delay functions exclusively one only loses some very fine details of the decay scenario. However, with the indicator function we only obtain information of the invariant sets that intersect the initial conditions chosen.

We used an indicator function to display information on the localized chaotic invariant set of the system. This reminds us of the inverse chaotic scattering problem, where we use scattering functions and in particular also the time delay function as an indicator function to obtain information on the localized chaotic invariant set by asymptotic measurements. The only difference is that in scattering problems we use as the domain of the indicator function a subset of asymptotic initial conditions. In this sense, we move this domain to an infinite distance and for compensation, we have to subtract from the time delay the trivial asymptotic contributions which diverge to infinity. Otherwise, we have a perfect analogy. For general information on chaotic scattering see chapter 6 in [19], [30], and chapter 4 in [31], for examples of the use of the time delay function in the inverse chaotic scattering problem see [32] and [33]. Our important new addition to this general basic idea archived in the present article is the special attention paid to tangential transient effects on unstable invariant subsets during their process of decay.

5 Acknowledgments

We thank DGAPA-UNAM for financial support under grant number IG101122 and CONAHCyT for financial support under grant number 425854. FGM thanks the Faculty of Mathematics and Physics of the University of Ljubljana for their hospitality during the last stage of this work.

References

- [1] S. Wiggins. *Normally Hyperbolic Invariant Manifolds in Dynamical Systems* (Springer Verlag, Berlin 1994).
- [2] N. Fenichel, Persistence and smoothness of invariant manifolds for flows, *Indiana Univ. Math. J.* **21**, 193 (1971).
- [3] P. Berger and A. Bounemoura. A geometrical proof of the persistence of normally hyperbolic submanifolds. *Dynamical Systems*, **28**, 4 567, (2013).
- [4] J. Eldering. *Normally Hyperbolic Invariant Manifolds. The noncompact case.* (Atlantis Press Paris, 2013).
- [5] F. Gonzalez, G. Drotos, C. Jung. The decay of a normally hyperbolic invariant manifold to dust in a three degrees of freedom scattering system. *J. Phys. A: Math. Theor.* **47**, 045101 (2014).
- [6] C.-B. Li, A. Shoujiguchi, M. Toda, T. Komatsuzaki. Definability of No-Return Transition States in the High-Energy Regime above the Reaction Threshold. *Phys. Rev. Lett.* **97**, 2 028302 (2006).
- [7] Manuel Iñarra, Jesús F. Palacián, Ana Isabel Pascual, J. Pablo Salas; Bifurcations of dividing surfaces in chemical reactions. *J. Chem. Phys.* **135** 1, 014110 (2011).
- [8] A. Allahem, T. Bartsch. Chaotic dynamics in multidimensional transition states. *J. Chem. Phys.* **137** 21, 214310 (2012).
- [9] F. A. L. Mauguière, P. Collins, G. S. Ezra, W. Wiggins. Bifurcations of Normally Hyperbolic Invariant Manifolds in analytical tractable models and consequences for reaction dynamics. *International Journal of Bifurcation and Chaos* **23**, 12 (2013).
- [10] H. Teramoto, M. Toda, T. Komatsuzaki. Dynamical Switching of a Reaction Coordinate to Carry the System through to a Different Product State at High Energies. *Phys. Rev. Lett.* **106**, 054101 (2011).
- [11] R. S. MacKay and D. C. Strub. Bifurcations of transition states: Morse bifurcations. *Nonlinearity* **27**, 859 (2014).
- [12] H. Teramoto, M. Toda, T. Komatsuzaki. Breakdown mechanisms of normally hyperbolic invariant manifolds in terms of unstable periodic orbits and homoclinic/heteroclinic orbits in Hamiltonian systems. *Nonlinearity* **28** 2677, (2015).
- [13] H. Teramoto, M. Toda, M. Takahashi, H. Kono, T. Komatsuzaki. Mechanism and Experimental Observability of Global Switching Between Reactive and Nonreactive Coordinates at High Total Energies. *Phys. Rev. Lett.* **115**, 093003 (2015).
- [14] M. Firmbach, A. Bäcker, R. Ketzmerick. Partial barriers to chaotic transport in 4D symplectic maps. *Chaos* **33**, 013125 (2023).
- [15] J. Stöber, A. Bäcker, and R. Ketzmerick Quantum transport through partial barriers in higher-dimensional systems. *Phys. Rev. Lett.* **132**, 047201, (2024)
- [16] J. Reiffa, J. Zatscha, J. Main, R. Hernandez. On the stability of satellites at unstable libration points of sun–planet–moon systems. *Commun. Nonlinear Sci. Numer. Simul.* **104**, 106053 (2022).
- [17] F. Gonzalez Montoya, C. Jung. The numerical search for the internal dynamics of NHIMs and their pictorial representation, *Physica D* **436**, 133330 (2022).
- [18] C. Jung. Transient effects in the decay of a normally hyperbolic invariant manifold. *J. Phys. Complex.* **2**, 014001 (2021).
- [19] Y.-C. Lai, T. Tél. *Transient Chaos: Complex Dynamics on Finite Time Scales.* (Springer New York, NY 2011).
- [20] F. Gonzalez, C. Jung. Visualizing the perturbation of partial integrability, *J. Phys. A: Math. Theor.* **48** , 43 (2015).
- [21] E. Lega, M. Guzzo, C Froeschlé. Theory and Applications of the Fast Lyapunov Indicator (FLI) Method. *Lecture Notes in Physics.* **915** (2016).
- [22] S. Wiggins, V. J. García-Garrido, Painting the Phase Portrait of a Dynamical System with the Computational Tool of Lagrangian Descriptors. *Notices of the American Mathematical Society* **69**, 936 (2022).
- [23] A. M. Mancho, S. Wiggins, J. Curbelo, C. Mendoza, Lagrangian Descriptors: A Method for Revealing Phase Space Structures of General Time Dependent Dynamical Systems. *Commun. Nonlinear Sci. Numer. Simul.* **18**, 3530 (2013).
- [24] C. Lopesino, F. Balibrea-Iniesta, V. J. García-Garrido, S. Wiggins, A. M. Mancho, A Theoretical Framework for Lagrangian Descriptors, *International Journal of Bifurcation and Chaos* **27**, 1730001 (2017).

- [25] J.D. Meiss, E. Sander. Birkhoff averages and the breakdown of invariant tori in volume-preserving maps. *Physica D* **428** 133048 (2021).
- [26] F. Gonzalez Montoya, The Classical Action as a Tool to Visualise the Phase Space of Hamiltonian Systems, *Dynamics*, **3**, 678 (2023).
- [27] M. Katsanikas, M. Agaoglou, F. González Montoya. Introduction to special issue: Chaos Indicators, Phase Space and Chemical Reaction Dynamics. *Physica D* **439** 133385 (2022).
- [28] C. Skokos, G. A. Gottwald, J. Laskar. *Chaos Detection and Predictability. Lecture Notes in Physics.* Springer Berlin, Heidelberg. (2016).
- [29] F. Gonzalez, C. Jung. Rainbow singularities in the doubly differential cross section for scattering off a perturbed magnetic dipole. *J. Phys. A: Math. Theor.* **45**, 265102 (2012).
- [30] J. M. Seoane , M.A.F. Sanjuan, New developments in classical chaotic scattering, *Rep. Prog. Phys.* **76**, 016001 (2013).
- [31] L. Reichl, *The Transition to Chaos: Conservative Classical and Quantum Systems*, 3rd edition, Springer 2021.
- [32] C. Jung, C. Lipp, T.H. Seligman, The Inverse Scattering Problem for Chaotic Hamiltonian Systems, *Annals of Physics*, **275**, 151 (1999).
- [33] H. Tapia and C. Jung, Inelastic inverse chaotic scattering problem, *Physics Letters A* **313**, 198 (2003).